LA-UR- 09-05560

Title: Computational studies of two-phase cement-CO2-brine interaction in wellbore environments

Author(s): James William Carey and Peter C. Lichtner

Intended for: SPE International Conference on CO2 Capture & Storage

SPE 126666

Computational studies of two-phase cement-CO_2-brine interaction in wellbore environments

J. William Carey and Peter C. Lichtner Los Alamos National Laboratory

This paper was prepared for presentation at the 2009 SPE International Conference on CO_2 Capture, Storage, and Utilization held in San Diego, California, USA, 2–4 November 2009.

Abstract

Wellbore integrity is essential to ensuring long-term isolation of buoyant supercritical CO_2 during geologic sequestration of CO_2. In this report, we summarize recent progress in numerical simulations of cement-brine-CO_2 interactions with respect to migration of CO_2 outside of casing. Using typical values for the hydrologic properties of cement, caprock (shale) and reservoir materials, we show that the capillary properties of good quality cement will prevent flow of CO_2 into and through cement. Rather, CO_2, if present, is likely to be confined to the casing-cement or cement-formation interfaces. CO_2 does react with the cement by diffusion from the interface into the cement, in which case it produces distinct carbonation fronts within the cement. This is consistent with observations of cement performance at the CO_2-enhanced oil recovery SACROC Unit in West Texas (Carey et al. 2007). For poor quality cement, flow through cement may occur and would produce a pattern of uniform carbonation without reaction fronts. We also consider an alternative explanation for cement carbonation reactions as due to CO_2 derived from caprock. We show that carbonation reactions in cement are limited to surficial reactions when CO_2 pressure is low (< 10 bars) as might be expected in many caprock environments. For the case of caprock overlying natural CO_2 reservoirs for millions of years, we consider Scherer and Huet's (2009) hypothesis of diffusive steady-state between CO_2 in the reservoir and in the caprock. We find that in this case, the aqueous CO_2 concentration would differ little from the reservoir and would be expected to produce carbonation reaction fronts in cements that are relatively uniform as a function of depth.

Introduction

Wellbore integrity signifies isolation of fluids in the subsurface. In the geologic sequestration of CO_2, this requires preventing the migration of buoyant, supercritical CO_2, a fluid that is highly mobile (a viscosity about $1/10^{th}$ that of water) and that is partially immiscible with brine and oil. Aqueous CO_2 forms by reaction of supercritical CO_2 and brine and generates an acidic solution (pH in the range of 4.5-5 in the presence of calcite) that is chemically reactive with the Portland cement and steel casing that provide isolation in most wellbore systems. Wellbore failure in the context of geologic sequestration is leakage that occurs through either primary defects (e.g., along a microannulus at the cement-casing interface) or through secondary defects induced by chemical degradation of the wellbore system. One of the key goals in the evaluation of the long-term safety and security of CO_2 sequestration is thus the determination of whether zonal isolation deteriorates or improves through chemical interactions with CO_2 in addition to calculation of the flux of CO_2 as a function of conditions in the wellbore environment.

Chemical reaction of CO_2 with Portland cement is complex and involves dissolution of portlandite [$Ca(OH)_2$]:

$$Ca(OH)_2 + 2CO_2 \rightarrow Ca^{2+} + 2HCO_3^- \qquad (1)$$

dissolution of calcium silicate hydrate [Ca_xSiO_{2+x}] which is the primary structural material in cement:

$$Ca_xSiO_{2+x} + xH_2O + 2xCO_2 \rightarrow xCa^{2+} + 2xHCO_3^- + SiO_2(aq) \qquad (2)$$

and the precipitation of calcium carbonate [$CaCO_3$]:

$$Ca^{2+} + 2HCO_3^- \rightarrow CaCO_3 + H_2O \qquad (3)$$

(e.g., Taylor 1990; Carey and Lichtner 2007). If reactions 1 and 2 predominate, the flux of CO_2 will increase with time as the cement sheath deteriorates. On the other hand, if precipitation of calcium carbonate is significant, CO_2 leakage pathways may self-seal and ultimately limit the flux of CO_2.

In this study, we summarize recent progress in developing numerical simulations of cement-brine-CO_2 interactions. The simulations were motivated by observations of cement performance at the CO_2-enhanced oil recovery SACROC Unit in West Texas (Figure 1; Carey et al. 2007) and by recent results from a natural CO_2 reservoir (Crow et al. 2008). The SACROC well was 55 years in age with 30 years of operation as a CO_2 producer and injector. Samples of cement from 3 meters above the reservoir-caprock interface showed reactions with CO_2 at both the casing and formation interfaces (see Carey et al. 2007 for more details). Preliminary 1-D diffusion-based models were able to reproduce the observed mineralogical changes at SACROC (Figure 2). In particular, the model reproduced the complete carbonation of the cement along a 0.5-cm reaction front adjacent to the caprock and the presence of a siliceous deposit at the interface between the carbonated (orange) and uncarbonated (gray) cement.

The Carey et al. model was limited in scope and assumed that CO_2 migrated along the cement-formation interface and then diffused into the cement. In this study, we examine other hypotheses for CO_2 leakage and compare these with the observations at SACROC. These include flow of CO_2 through cement, diffusion of CO_2 through the caprock and subsequent reaction with cement, and flow along the cement-formation interface.

Methods. In our study of CO_2-cement reactions, we have applied two versions of a flow and reactive transport code developed at Los Alamos: FLOTRAN (Lichtner 2003) and PFLOTRAN (v. 1; Lu and Lichtner 2005). Both codes use the Span and Wagner (1996) equation of state for CO_2 with dissolved CO_2 obtained from Duan and Sun (2003). Chemical reactions consist of aqueous speciation assumed to be in local equilibrium and mineral precipitation and dissolution described through kinetic rate laws. All mineralogical reactions with CO_2 occur through dissolved CO_2 in the brine phase. PFLOTRAN is a parallelized version of FLOTRAN. Parallelization is based on domain decomposition using the PETSc parallel framework. The code consists of two separate modules, PFLOW describing multiphase fluid flow and PTRAN describing reactive transport. The two modules are sequentially coupled using linear interpolation to obtain the fluid velocity, phase saturation, temperature and pressure at intermediate time steps. While FLOTRAN accurately characterizes the solubility of CO_2 in equilibrium with supercritical CO_2, it does not have the capability of representing saturation and flow of the supercritical CO_2 phase; PFLOTRAN has the capability of fully representing the properties of multiphase flow and reaction of supercritical CO_2.

In previous studies, we used a detailed representation of cement mineralogy that included a solid-solution model for calcium silicate hydrate (CSH; Carey and Lichtner 2007) in addition to other cement phases including hydrogarnet, monosulfate, ettringite, and portlandite. While these details are useful, we have found that in the interest of computational simplicity, CSH can be represented as a pure phase. In other cases described below, we simplified the cement further to consist solely of portlandite. The thermodynamic and kinetic properties of cement and formation rocks are as given in Carey and Lichtner (2007).

Flow and reaction of supercritical CO_2 through cement. Diffusion of CO_2 through cement is a slow process and can lead to relatively narrow carbonation zones (~1 cm) over periods as long as 30 years (Figure 1 and 2). An alternative leakage scenario consists of flow of CO_2 through cement which is likely to be significantly more rapid than diffusion. However, CO_2 must displace water from the cement and the extent of infiltration is a function of the relative capillary properties of the cement, the interface zone, and the caprock material as well as any pressure gradient imposed on the system by buoyancy of the CO_2 plume or other hydrologic gradients.

Typical capillary pressure properties of cement, caprock (shale), and a reservoir material are illustrated in Figure 3 and summarized in Table 1. These are derived from experimental studies and show that both fresh, unaltered cement and shale have very high capillary entry pressures, requiring an over-pressure greater than 100 bars (or >1000 m of supercritical CO_2 assuming a density contrast of 0.3 g/cm^3). This is in contrast to the properties of a sandstone reservoir rock in which entry pressures are less than 0.1 bars. In comparison with shale, Portland cement shows greater resistance to the displacement of water as saturation decreases. These results indicate that cement will resist the displacement of pore water to very high pressure gradients.

1-D capillary displacement results. The impact of capillary pressure relations were investigated in 1-D calculations in which brine-saturated cement (5 cm in width) is initially in contact with either reservoir rock or caprock shale (20 cm in width) containing a 50:50 mixture of supercritical CO_2 and brine. The 1-D problem was discretized into 400 cells of size varying from 0.00025-0.002 m. Temperature and pressure were 50 °C and 220 bars. In these calculations, the only driving forces for CO_2 movement into cement are by diffusion and capillary drainage of the cement. These calculations were conducted without chemical reactions other than dissolution of CO_2 into the brine. Simulations were conducted for a 1 year time period (compare Figure 2 which is 30 years). The results were characterized in terms of saturation of supercritical CO_2 and the concentration of aqueous CO_2 as a function of time.

The simulations were designed to investigate how the contrast in capillary properties between the cement and the formation rock containing CO_2 influences the extent of CO_2 penetration in the cement. Within the reservoir, cement will be in contact with rock having strongly contrasting capillary properties (Figure 3). Because the interface between cement and formation is vertical for a non-deviated well, there is no hydraulic pressure gradient across the interface and CO_2 flow can only be driven by capillary forces. As a result, there is essentially no flow from the reservoir into the cement (Figure 4). However, diffusion allows some aqueous CO_2 to penetrate the cement (Figure 5).

If supercritical CO_2 is present in a shale caprock, the contrast in capillary properties between cement and shale are much smaller. In this situation, there is again no pressure difference between the cement and shale and flow occurs only by capillary pressure. With a shale source, a limited quantity of CO_2 flows into the cement leading to saturation levels of a few % CO_2 after 1 year (Figure 6). The penetration of supercritical CO_2 into the cement leads to much higher concentrations of aqueous CO_2 (Figure 7). After 1 year, almost the entire 5 cm region of cement is fully saturated with aqueous CO_2.

1-D capillary flow and reaction results. In this section, we examine the mineralogical reactions resulting from the differing capillary displacement patterns. In these calculations, we used the same 1-D grid and material properties presented previously but extend the calculations to 30 years. The cement mineralogy was represented with 54% calcium-silicate-hydrate, 22% portlandite, 29% calcium alumino-sulfate (monosulfate), and 5% hydrogarnet. The cement had an initial porosity of 40%. The formation rock had 20% porosity with a mineralogy that included quartz, albite, illite, kaolinite, calcite, and dolomite. Of these, only the carbonates are significantly reactive over the 30 year calculation. Mineral reaction rates were the same as used by Carey et al. 2007 (Figure 2).

For cement in contact with a rock with reservoir-like capillary pressure properties, CO_2 enters only through aqueous diffusion (c.f., Figures 4 and 5) with the result that a distinct reaction front occurs (Figures 8 and 9). After one year of simulated time, the cement is only partially carbonated in a 1-cm zone adjacent to the reservoir rock. The remainder of the cement is unaltered. After 30 years, the carbonation front has moved 3-cm into the cement.

For cement in contact with a formation rock with shale-like capillary properties, penetration of CO_2 into the cement occurs (cf., Figures 6 and 7). This results in a uniform carbonation pattern in which carbonate is present throughout the cement (Figures 9 and 10). There is no distinct carbonation front resulting from CO_2 flow into cement.

Implications of 1-D capillary flow results. The 1-D simulations show that the relative capillary-pressure properties of the cement and the formation rock containing CO_2 have a very significant impact on the character of the CO_2 reactions with the cement. For unaltered cement with high capillary pressure properties, CO_2 can only penetrate via diffusion from rocks that have substantially lower capillary pressure curves, as is typical for most reservoir rocks. The resulting pattern of mineralogical alteration includes a distinct reaction front and the preservation of unaltered cement. In contrast, CO_2 can penetrate cement in contact with shale due to the similarity in capillary properties.

These results would appear to be inconsistent with the SACROC samples, since the cement was recovered 3 m above the reservoir and adjacent to the shale caprock. However, the interface between the cement and shale caprock was not a tight bond but rather a disturbed zone of rock fragments (filter cake). As a consequence, this interface had properties that were more likely similar to sandstone or other permeable, porous material and was thus a region with minimal capillary suction. Supercritical CO_2 within this region would not have invaded the cement except by diffusion. In the case of diffusion, the numerical models predict a band of carbonation separated from relatively unaltered cement, a pattern that is readily seen in the orange carbonation zone of Figure 1. Indeed, the fact that the reaction front between carbonated and uncarbonated cement was parallel to the casing-cement interface shows that CO_2 migrated from the interface into the cement. This CO_2 must have traveled up the interface from the reservoir while diffusing into the cement along its path rather than having permeated the cement from the base of the reservoir.

These observations can be generalized. In wellbore systems with cement having good hydrologic properties, there are few scenarios in which supercritical CO_2 would flow through the cement. The CO_2 would not move from rocks with reservoir-like properties to enter cement. If CO_2 were present in the caprock and there was a good bond between caprock and cement, then it is possible that CO_2 would enter the cement (Figure 6). However, supercritical CO_2 is unlikely to be present in the caprock due to its low permeability and capillary resistance, and is more likely to migrate along interfaces which are open regions that it is unlikely to leave. Carbonation of good quality cement should therefore occur only by diffusion of CO_2 from interfaces into the cement.

Carbonation of wellbore cement due to CO_2-bearing caprock

Scherer and Huet (2009) have suggested an alternative explanation for observations of carbonation of wellbore cement in a natural CO_2 reservoir (Crow et al. 2009). They provide an analysis of diffusion of CO_2 from the reservoir into the caprock and subsequent reaction with the wellbore. In this account, carbonation of wellbore cement does not necessarily occur due to migration of CO_2-bearing fluids along wellbore interfaces, but rather that geologic time would allow a diffusive steady state between the CO_2 in the reservoir and the overlying caprock. In such an environment, diffusive carbonation reaction fronts in cement (Figure 1) may be due to diffusion of CO_2 from the caprock and not an indicator of a lack of wellbore integrity. In this section, we extend Scherer and Huet's analysis by using reactive transport calculations to evaluate the distribution of CO_2 within the caprock and the likely pattern of cement carbonation resulting from such a distribution. We divide the analysis into two questions: do lower CO_2 pressures in the caprock result in distinct carbonation patterns in cement? And what is the distribution of CO_2 within reactive caprock in diffusive equilibrium with the reservoir?

Effect of CO_2 pressure. Simulations were performed on a 400-cell 1-D grid as before but with a highly simplified mineralogy. The cement was represented by portlandite and the caprock by a mixture of quartz and calcite. While some of the mineralogical complexity is missing from this model, it captures the essential features of an alkaline reactive material (cement) adjacent to a calcite-bearing caprock. As in the previous section, diffusion is taken as the dominant CO_2 interaction process with cement. The porosity/tortuosity of the cement and formation rock are 0.35/0.004 and 0.25/0.1 respectively; temperature is 40 °C.

The effect of CO_2 pressure in the caprock was investigated at 10^{-3}, 1, 10, and 100 bars for simulations over a 30-year time period. The results are presented in terms of portlandite dissolved and calcite precipitated (Figure 12). These show that diffusion and reaction of CO_2 in cement is limited at pressures below 10 bars. Thus we would not expect that low background levels of CO_2 associated with the simple presence of carbonate in caprocks would produce only a small degree of surficial carbonation of cement. Significant carbonation, as observed at SACROC, requires a significantly elevated CO_2 pressure.

CO_2 concentration in caprock. Scherer and Huet (2009) observe that geologic time would allow supercritical CO_2 in the reservoir to come to diffusive steady state with the overlying caprock. They assumed a tortuosity in the shale of 0.01 and calculated steady state conditions in a 40 m caprock after 1.6 million years. In their model, they hypothesized that reaction of CO_2 with calcite in strata overlying the caprock would result in a very low CO_2 concentration at the top of the caprock. In this section, we examine this hypothesis and evaluate CO_2 concentration and pressure within caprock connected to a supercritical CO_2-bearing reservoir rock. The simulations were conducted on a 400-cell, 1-D grid with length of 3.5 m. Sandstone consisting of 60% quartz and 10% calcite occupied the region from 0-0.25 m and had porosity and tortuosity of 30% and 0.1. The shale caprock consisted of 75% quartz and 10% calcite and occupied the remainder of the region from 0.25 to 3.5 m. It had a porosity and tortuosity of 15% and 0.01. The sandstone was in equilibrium with 100 bars of CO_2 pressure and the shale was initially at a CO_2 pressure of 10^{-3} bars. The temperature was 40 °C and the calculations were conducted to 1,000 years.

The effect of reactions with calcite on the diffusion of CO_2 into shale is mixed (Figures 13 and 14). The depth of aqueous CO_2 migration and the associated CO_2 pressure are not significantly affected by chemical reactions with calcite. This appears to be the case because the concentration of diffusing CO_2 is much larger than quantities consumed by calcite dissolution reactions with CO_2. The pH (and Ca concentration), on the other hand, is delayed by reaction with calcite.

Although these calculations were conducted for a 1,000 year period for only a 3.5 m section, the results can be extrapolated to greater times and distances. The calculations clearly show that reactions with calcite have no significant impact on CO_2 concentrations. For example, at the distance 0.5 m in the shale (Figure 13) calcite is in equilibrium with a CO_2 concentration that is essentially the same as in the reservoir. If as Scherer and Huet (2009) suggest, caprock is in diffusive steady state with a supercritical CO_2-bearing reservoir, the concentration of aqueous CO_2 in the caprock would approach values similar to that in the reservoir itself. As a consequence, wellbore cement adjacent to caprock would be exposed to high-pressure CO_2 and would presumably develop significant carbonation reaction fronts (Figure 12). The pattern of carbonation in the cement in such a scenario would be such that the entire wellbore column would show rather uniform carbonation reaction fronts.

As aqueous CO_2 migrates into the shale, it is accompanied by an increase in the effective CO_2 pressure within the shale. This would not necessarily result in the appearance of separate phase supercritical CO_2 at least to the extent that hydrostatic pressure within the caprock is capable of containing the pressure. Thus elevated CO_2 concentrations in caprock may not be detected as gas saturation. However, fluid samples recovered from the shale would be CO_2-rich and provide an alternative method for evaluating caprock storage capacity.

Conclusions

Our study was motivated by observations of carbonated cement recovered from wellbores in analog sites for the geologic sequestration of CO_2. We examined three hypotheses for the origin of CO_2 resulting in carbonation: migration along wellbore interfaces, flow through cement, and diffusion from CO_2-bearing caprock. Our numerical results indicate that supercritical CO_2 will not flow through good quality cement due to the capillary properties of cement. In this case, leakage of CO_2 is confined to wellbore interfaces and carbonation of cement occurs by diffusion of CO_2 into the cement from the interface. In addition, carbonation by diffusion creates reaction fronts that are distinct from the uniform carbonation pattern generated by flow of CO_2 through cement. Diffusion of CO_2 from the caprock will not significantly carbonate the cement unless the CO_2 pressure is relatively high (> 10 bars). This could be the case in caprock above natural CO_2 reservoir which have had millions of years to reach diffusive steady state. In such an environment, the entire wellbore sheath would show a similar extent of carbonation reaction fronts due to the relatively uniform CO_2 concentration in the caprock.

Acknowledgements. The authors express gratitude to the Department of Energy Fossil Energy (program 04FE04-09) and the CO_2 Capture Project for financial support.

References

Bennion, B. and Bachu, S. (2006) The impact of interfacial tension and pore-size distribution/capillary pressure character on CO_2 relative permeability at reservoir conditions in CO_2-brine systems. Proceedings - SPE Symposium on Improved Oil Recovery 1: 142–151.

Carey, J. W. and Lichtner, P. C. (2007) Calcium silicate hydrate (C-S-H) solid solution model applied to cement degradation using the continuum reactive transport model FLOTRAN. In Mobasher, B. and Skalny, J., editors, Transport Properties and Concrete Quality: Materials Science of Concrete, Special Volume, pp. 73-106. American Ceramic Society: John Wiley & Sons, Inc.

Carey, J. W., Wigand, M., Chipera, S., WoldeGabriel, G., Pawar, R., Lichtner, P., Wehner, S., Raines, M., and Guthrie, G. D., Jr. (2007e) Analysis and performance of oil well cement with 30 years of CO2 exposure from the SACROC Unit, West Texas, USA. International Journal of Greenhouse Gas Control 1: 75-85.

Crow, W., Williams, B., Carey, J. W., Celia, M., and Gasda, S. (2008) Wellbore integrity analysis of a natural CO2 producer. In Energy Procedia: 9th International Conference on Greenhouse Gas Control Technologies, vol. 1, pp. 3561-3569.

Duan, Z. and Sun, R. (2003) An improved model calculating CO_2 solubility in pure water and aqueous NaCl solutions from 273 to 533 K and from 0 to 2000 bar. Chemical Geology 193: 257–271.

Lichtner, P. C. (2001) FLOTRAN User Manual. Technical Report LA-UR-01-2349, Los Alamos National Laboratory, 168 pp.

Lu, C. and Lichtner, P. C. (2005) PFLOTRAN: Massively parallel 3-D simulator for CO_2 sequestration in geologic media. In Fourth Annual Conference on Carbon Capture & Sequestration, May, 2005, Alexandria, VA.

Savage, B. M. and Janssen, D. J. (1997) Soil physics principles validated for use in predicting unsaturated moisture movement in Portland cement concrete. ACI Materials Journal 94: 63–70.

Scherer, G. W. and Huet, B. (2009) Carbonation of wellbore cement by CO_2 diffusion from caprock. International Journal of Greenhouse Gas Control (in press).

Span, R. and Wagner, W. (1996) A new equation of state for carbon dioxide covering the fluid region from the triple-point temperature to 1100 K at pressures up to 800 MPa. Journal of Physical and Chemical Reference Data 25: 1509–1596.

Taylor, H. F. W. (1990) Cement Chemistry. Academic Press, London, 475 pp.

Table 1. Summary of hydrologic properties of cement, shale, and reservoir rock used in the simulations. Relative permeability relations were calculated using a van Genuchten capillary pressure formulation: $\Psi = \alpha^{-1}(S^{-\frac{1}{m}} - 1)^{m-1}$, where S is the saturation and m and α are fit parameters. Simulations were conducted at 50 °C and with a CO_2 pressure of 200 bars.

	Perm (mD)	α	m	φ	τ
Cement	0.1	0.0023	0.42	0.4	0.005
Shale	0.1	0.01	0.9	0.2	0.5
Reservoir	100	10	0.5	0.2	0.5

Permeability given in milliDarcy (mD); φ is porosity; τ is tortuosity.

Figure 1. Polished face of cement recovered from a wellbore at the SACROC Unit in west Texas. Orange alteration reflects carbonation from fluids migrating along the cement-caprock interface on the right side of the image (about 5 cm in length). A narrow, dense, siliceous deposit separates the orange altered cement from relatively unaltered gray cement (from Carey et al. 2007).

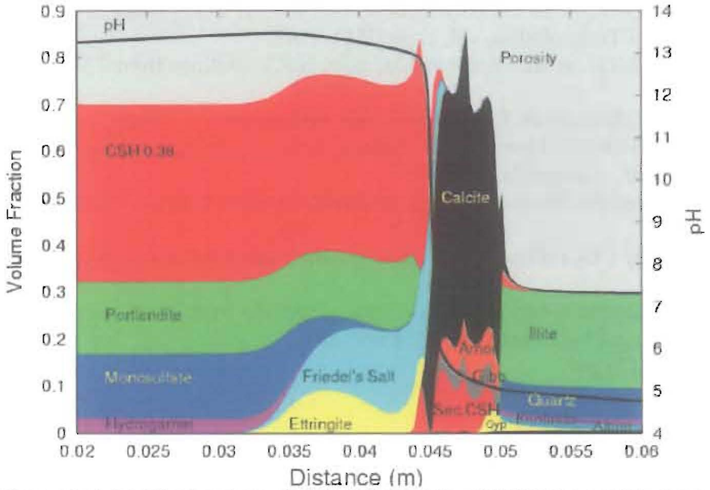

Figure 2. 1-D diffusion-based simulation of the SACROC cement observations. A 0.5 cm zone of calcite + amorphous silica replaces the cement at the cement-caprock interface (from Carey et al. 2007).

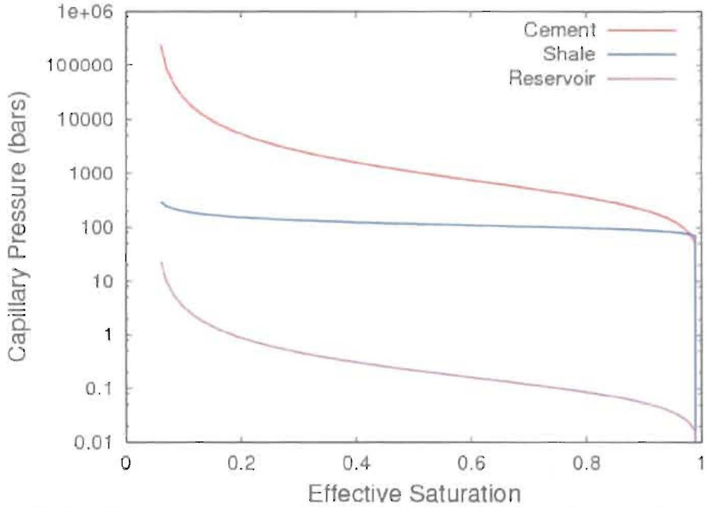

Figure 3. Capillary pressure curves for cement, shale, and reservoir rock (based on Bennion and Bachu, 2006 and Savage and Janssen, 1997). Saturation is the fraction of water occupying the porosity.

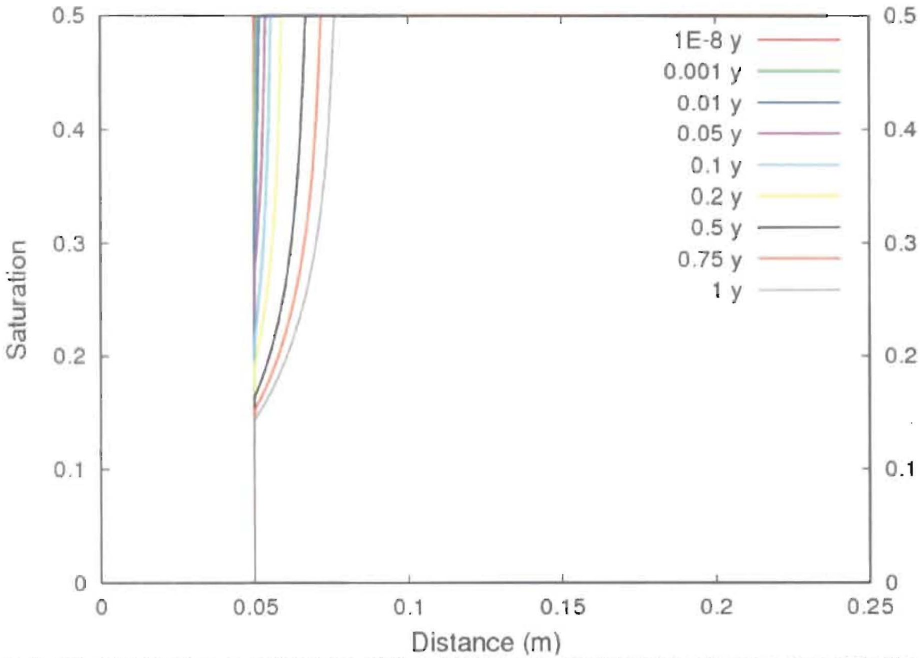

Figure 4. CO_2 distribution as a function of time between cement (0-0.05 m) and a reservoir-like rock with an initial 50% CO_2 content. CO_2 does not penetrate the cement. CO_2 saturation decreases at the cement/reservoir interface as it diffuses into the cement and water moves from the cement into the reservoir.

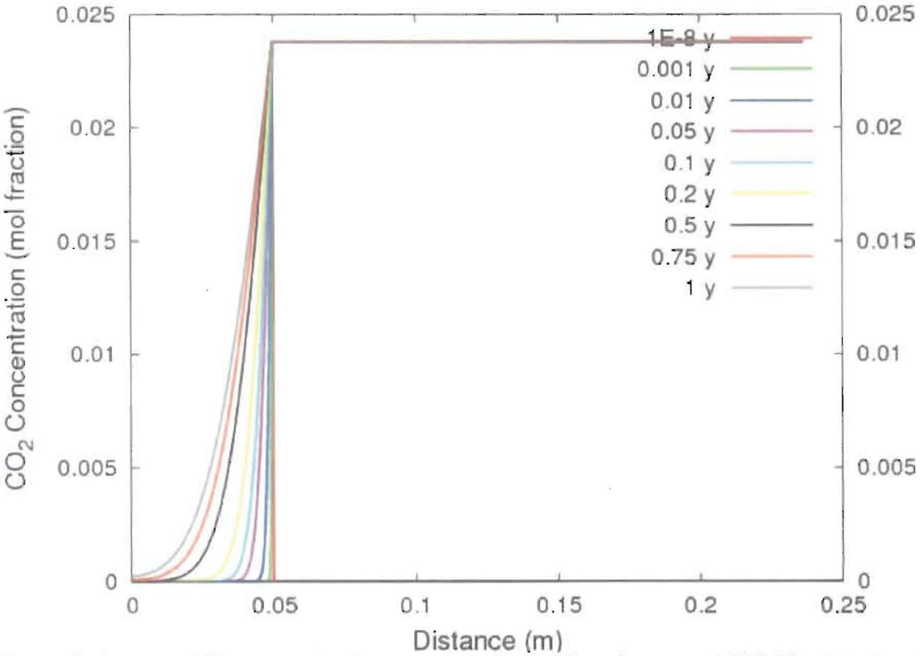

Figure 5. Aqueous CO_2 concentration as a function of time in cement (0-0.05 m) and a reservoir-like rock with an initial 50% CO_2 saturation. CO_2 enters the cement only through diffusion (cf., Figure 4).

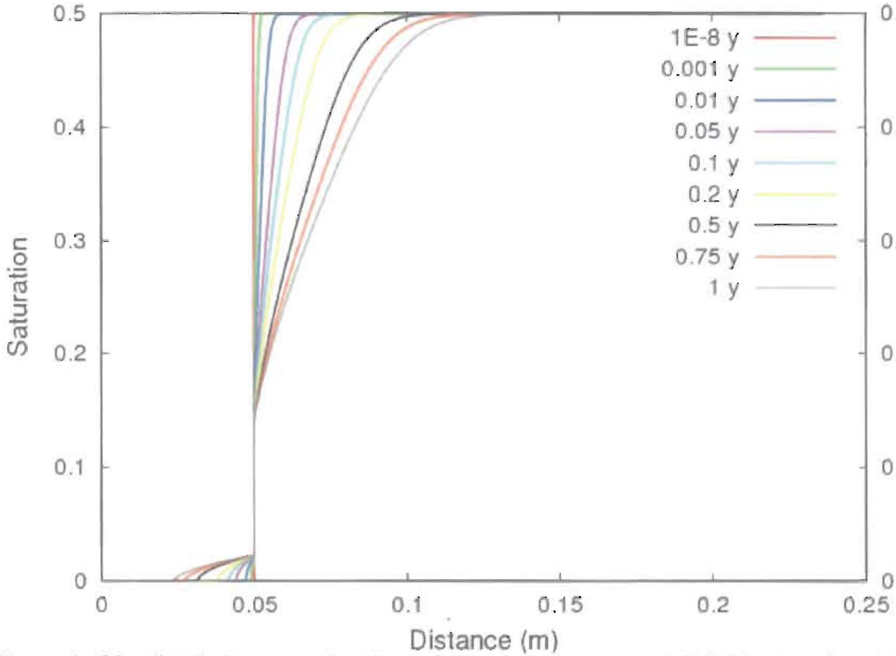

Figure 6. CO_2 distribution as a function of time between cement (0-0.05 m) and a shale formation rock with an initial 50% CO_2 content. Supercritical CO_2 enters the cement to a limited extent. CO_2 is lost from the caprock adjacent to the cement as it moves into the cement and water moves from the cement into the reservoir.

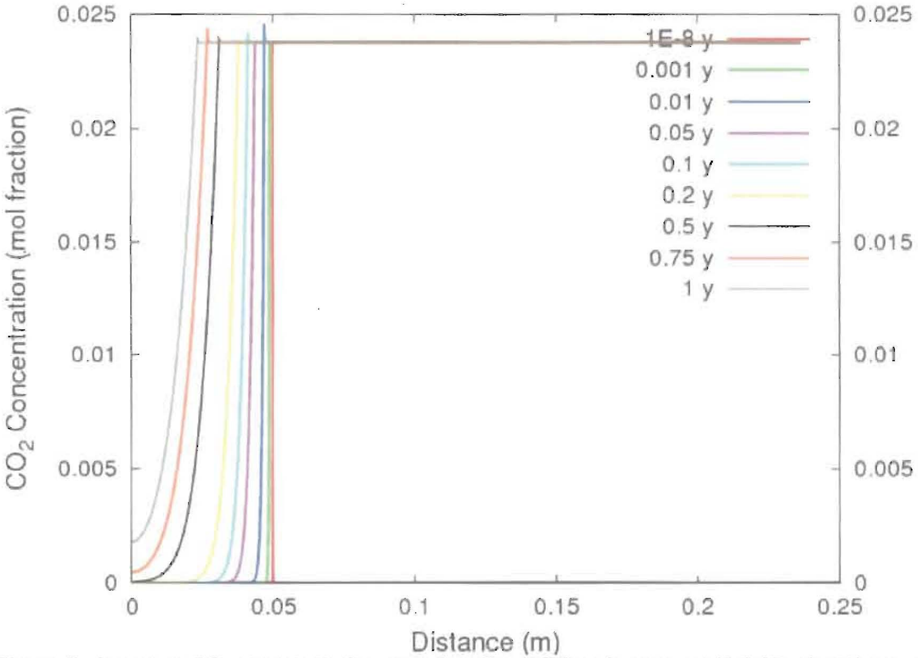

Figure 7. Aqueous CO_2 concentration as a function of time in cement (0-0.05 m) and a caprock-like rock (shale) with an initial 50% CO_2 saturation. The aqueous CO_2 concentration is at a maximum where supercritical CO_2 has penetrated the cement (cf., Figure 6).

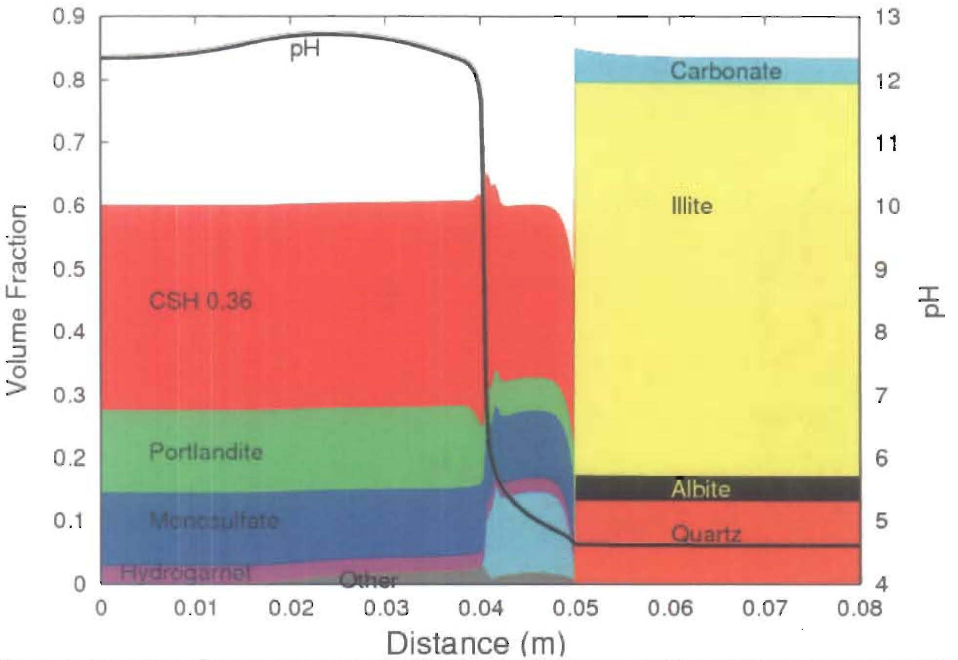

Figure 8. Reaction of cement in contact with a rock with reservoir-like capillary properties and 50% initial CO_2 saturation after 1 year. The reaction front penetrates about 1 cm and the cement is only partially altered in the reacted region.

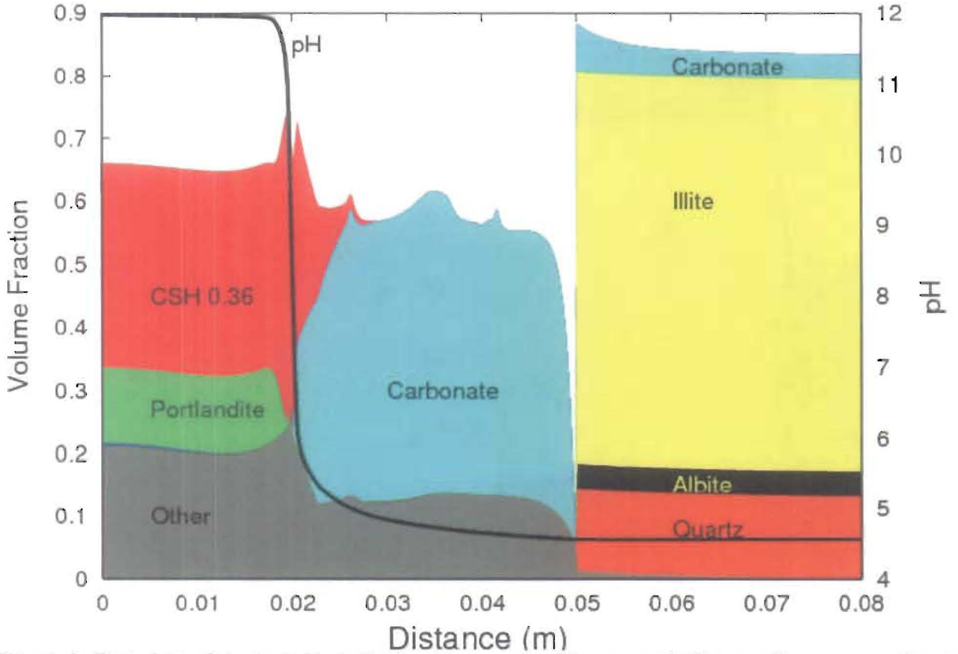

Figure 9. Reaction of cement in contact with a rock with reservoir-like capillary properties and 50% initial CO_2 saturation after 30 years. The reaction front penetrates about 3 cm and the interior of the cement is almost unmodified.

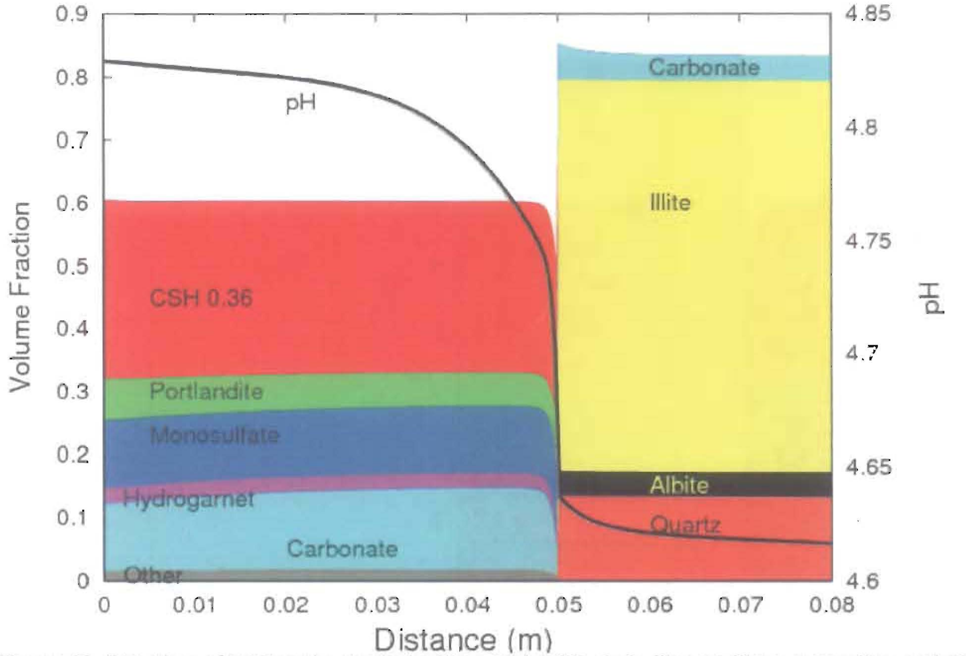

Figure 10. Reaction of cement in contact with a rock with shale-like capillary properties and 50% initial CO_2 saturation after 1 year. There is no reaction front and a uniform carbonation level characterizes the cement.

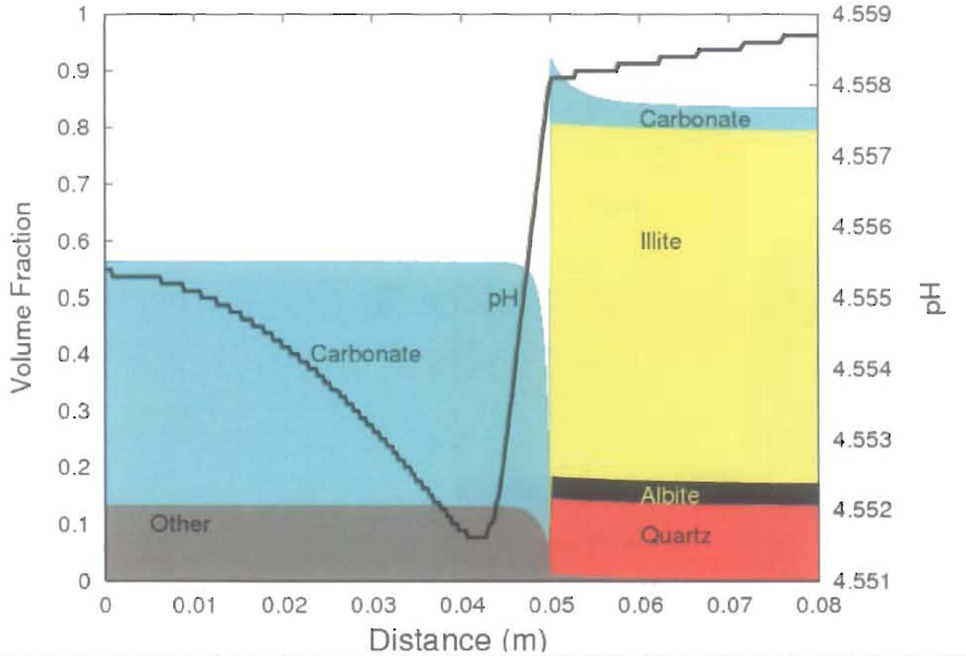

Figure 11. Reaction of cement in contact with a rock with shale-like capillary properties and 50% initial CO_2 saturation after 30 years. The cement is completely and uniformly carbonated.

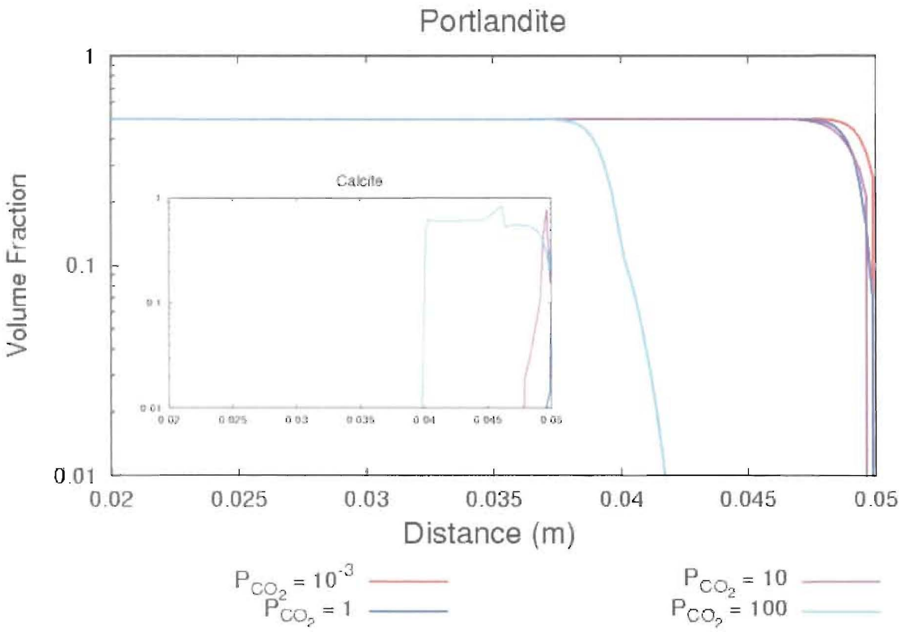

Figure 12. Diffusion and reaction of CO_2 with a simplified cement consisting of portlandite. The cement extends from 0-0.05 m and initially has no CO_2. The caprock is not illustrated but extends from 0.05 to 0.25 m and contains calcite in equilibrium with CO_2 of 4 differing pressures. Diffusion of CO_2 into the cement dissolves the portlandite and results in precipitation of calcite (inset).

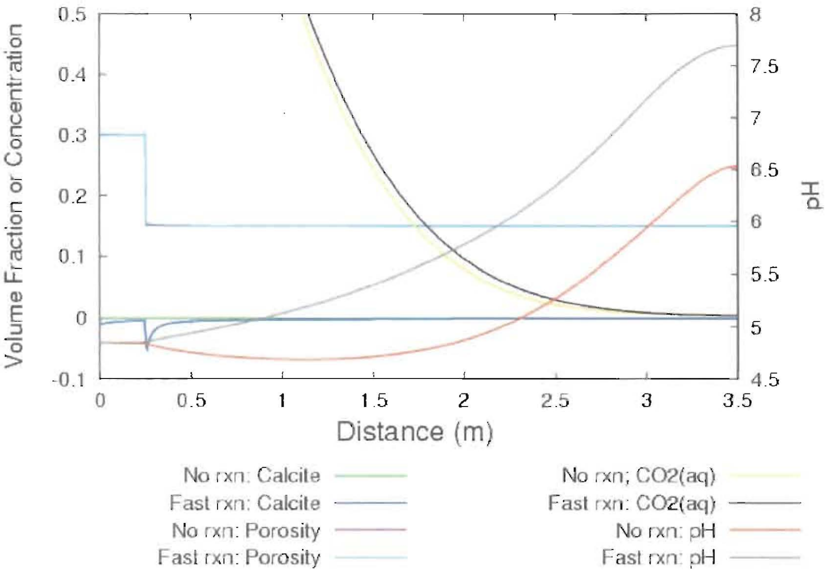

Figure 13. Compositional profile across sandstone reservoir (left of dotted line) with CO_2 and caprock (right of dotted line) which initially lacks CO_2 after 1,000 years of diffusional equilibration. Two cases are considered: reaction of calcite and CO_2 and no reaction. The calcite abundance is plotted as the difference between the starting concentration (0.1) multiplied by 10.

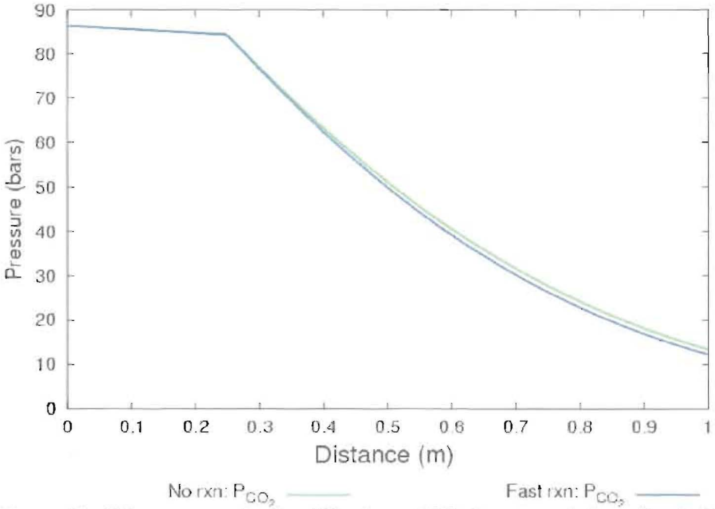

Figure 14. CO_2 pressure in the diffusion of CO_2 from sandstone (to right of dotted line) into shale (left of dotted line) at 1000 years.